

Effects of Turbulence Intensity on Gaseous Diffusion around Two Model Buildings

Masaaki OHBA*, Nobuyuki KOBAYASHI*

Wind tunnel experiments are conducted to investigate the effects of the turbulence intensity of a oncoming flow on the gaseous diffusion around two buildings. In the experiments, the turbulence intensity of the oncoming flow is varied by setting a mesh grid on the upstream of the measured section in the wind tunnel. Air flow characteristics such as mean velocity, turbulence intensity and wake length are measured by a hot-wire anemometer, and concentration distributions around models are investigated by a hydrocarbon analyzer using ethylene gas as tracer gas.

From the experiments, the following conclusions are confirmed. As the turbulence intensity of the oncoming flow increases, the concentrations on the rooftop of the low-rise model increases, while the concentrations on the ground surface between the models and on the upwind face of the high-rise model decreases. The length of cavity wake is also proportional to the turbulence intensity, and it is approximately 4 H for $\sqrt{u_0^2}/\bar{U}_0=15.3\%$.

List of Symbols

L: distance between model and mesh grid
H: height of low-rise model
 \bar{U} : mean wind velocity at height of Z
 \bar{U}_0 : mean wind velocity of oncoming flow at height Z=200 mm (reference wind velocity)
u: turbulence velocity
 $\sqrt{u^2}$: standard deviation of turbulence velocity u
 $\sqrt{u^2}/\bar{U}$: turbulence intensity
 $\sqrt{u_0^2}$: standard deviation of turbulence velocity u at reference height
 K_0 : reference turbulence diffusivity at reference height
 $(K_0 = \sqrt{u_0^2} \cdot \bar{U}_0 \cdot \int_0^{\tau_0} R(\tau) d\tau)$
 τ_0 : time length passed until $R(\tau)=0$

$R(\tau)$: autocorrelation coefficient

C_i : concentration of sampled gas

C_b : concentration of oncoming air in wind tunnel

C_0 : reference concentration [$C_0 = q/H^2\bar{U}_0$]

C_{*i} : dimensionless concentration [$C_{*i} = (C_i - C_b)/C_0$]

q: rate of tracer gas emitted from source of low-rise model

\bar{V}_g : emission velocity of tracer gas

N: number of sampled data

E_c : dimensionless concentration difference

$E\bar{U}$: dimensionless wind velocity difference

E_u : dimensionless turbulence velocity difference

1. INTRODUCTION

Wind tunnel experiments are very often conducted to investigate the environmental assessment on the gaseous diffusion around the district heating plants and the electric

* Asst. Professor, Department of Architecture, Faculty of Engineering, Tokyo Institute of Polytechnics

power plants which emit much gas from the stacks into the atmosphere^{1~4}). The most valuable information about air pollutions is given from the experiments. In order to simulate the gaseous diffusion around models in the wind tunnel, both Reynolds and Froude numbers in scaling criteria for the experiments, must coincide between prototypes and models, which is, however, very difficult.

Then, the relaxation of similarity criteria is taken for the dispersion of the gas which has buoyancy^{4~7}). It has reported that there is the region in which flow patterns are similar with any of Reynolds number. Therefore, the wind velocity in the wind tunnel is determined to ensure the minimum Reynolds number, which is in the range from 10,000 to 14,000 on cubic models^{8,9}).

However, when the turbulence intensities of the oncoming flow are different each other under the condition that the flow satisfies the minimum Reynolds number, the gaseous diffusion around models is not similar. Therefore, the minimum Reynolds number should be determined by considering the effect of the turbulence intensity of the oncoming flow.

This report, as the first step of the study, describes the effect of the turbulence intensity on gaseous diffusion and wind velocity distributions around two models. In the experiments, the turbulence intensity of the oncoming flow is varied by setting a mesh grid on the upstream of the measured section in the wind tunnel, and the Reynolds number, which is ensured to

be more than the minimum Reynolds number required, is kept constant. These data from the experiments ensure the importance of the turbulence for gaseous diffusion¹⁰).

2. OUTLINE OF WIND TUNNEL EXPERIMENTS

2.1 Wind tunnel

Figure 1 shows the wind tunnel used in the experiments. It is an open circuit type with two test sections and a traverse system to carry measuring probes in the test section II. The tunnel air is driven by a fan with a 7.5 kW thyristor-controlled DC motor.

The test section I used for the measurement of wind loading forward buildings is 0.7 m wide, 0.5 m high and 4.0 m long. The wind velocity is controlled from 0.5 m/s to 21 m/s.

The test section II used in the experiments is 1.2 m wide, 1.0 m high and 10 m long. The traverse system can travel 1.0 m in the x-direction, ± 0.5 m from the center in the y-direction, and 0.8 m from the floor in the z-direction. It is driven by a pulse motor with an accuracy of ± 0.1 mm. The wind velocity is controlled from 0.5 m/s to 6.0 m/s.

2.2 Building models

Two building models are used in the experiments. Figure 2 shows the configuration of the models. The low-rise model is 180 mm wide, 60 mm high and 60 mm long with the source in the center of the rooftop emitting the tracer gas. The diameter of the source size is 6 mm ($=H/10$). The high-rise model is

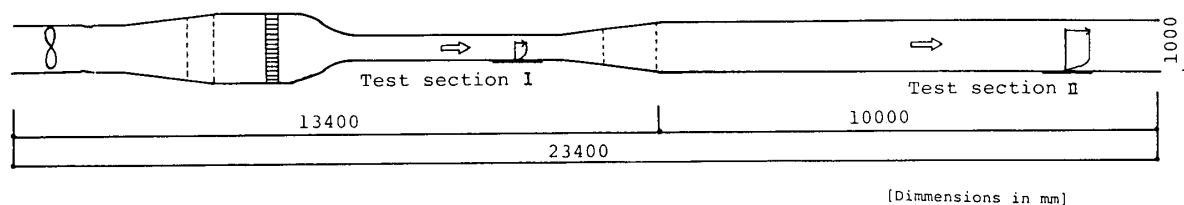


Fig. 1 Wind tunnel

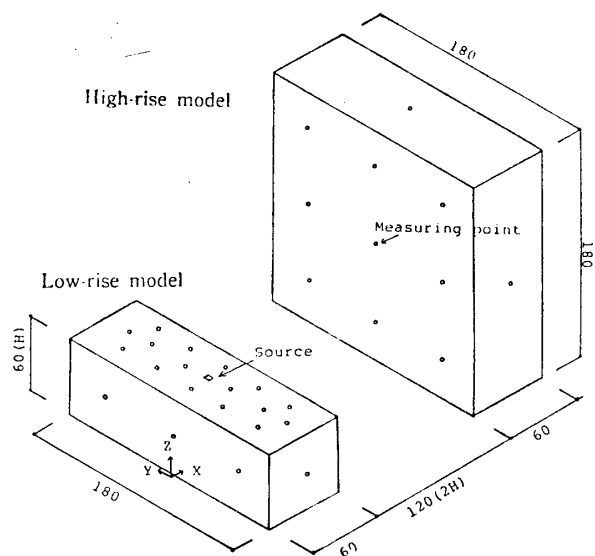


Fig. 2 Building models

180 mm wide, 180 mm high and 60 mm long. These two models are set perpendicular to the main flow. The distance between them is 120 mm ($=2H$).

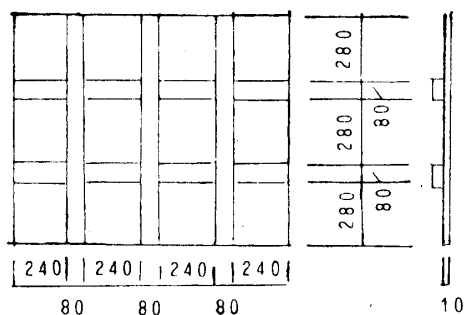


Fig. 3 Dimension of mesh grid

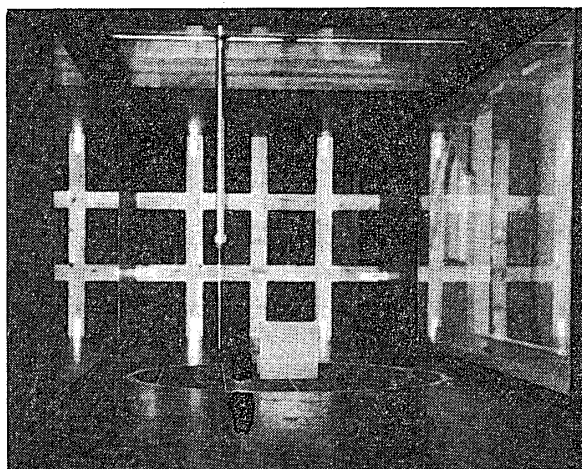


Fig. 4 Photo of models and mesh grid set in wind tunnel

2.3 Mesh grid

Figure 3 shows the configuration of the mesh grid. The ratio of the opened area to the cross-section area ($1.2 \text{ m} \times 1 \text{ m}$) is 0.33. Fig. 4 shows the models and the mesh grid set on the floor of the wind tunnel.

2.4 Measuring points

(1) Concentration measurement

There are 87 measuring points, among which 22 and 13 points are located on the low-rise and high-rise model surfaces respectively, and 52 are on the floor of the wind tunnel. The diameter of the sampling points is 2 mm.

(2) Wind velocity measurement

There are 203 measuring points, among which 117 and 86 points are pointed for the horizontal measurement at the height of 6 mm ($=H/10$) and for the vertical measurement along $Y/H=0$ respectively. Points are distributed densely around corners of the models.

2.5 Experimental conditions

Experimental conditions are listed in Table 1. Four experimental types are conducted by the wind tunnel experiments.

Table 1 Experimental data

No.	L	\bar{U}_0	$\sqrt{\overline{u^2}_0}/\bar{U}_0$	K_0	$\bar{V}g/\bar{U}_0$
1	2m	2.94 m/s	15.3%	0.070 m ² /s	0.05
2	3m	2.98 m/s	9.4%	0.046 m ² /s	0.05
3	5m	2.97 m/s	7.1%	0.034 m ² /s	0.05
4	without grid	2.96 m/s	6.8%	0.029 m ² /s	0.05

(1) Condition of oncoming flow

The vertical wind velocity profile of the oncoming flow is kept uniform. The reference velocity at the height $Z=200 \text{ mm}$ remains 3 m/s in order to ensure the minimum Reynolds number required. The turbulence intensities of the oncoming flow are varied by adjusting the position of the mesh grid, and taken in

the range of 6.8% to 15.3%. The turbulence diffusivity is proportional to $\sqrt{u_0^2}/\bar{U}_0$, and varied from 0.029 m²/s to 0.070 m²/s. Figure 5 shows the vertical wind velocity and turbulence intensity profiles. The maximum turbulence intensity, $\sqrt{u_0^2}/\bar{U}_0$, is 15.3% at the height $Z=200$ mm when the distance L is equal to $2H$.

(2) Condition of tracer gas emission rate

Ethylene gas is used as the tracer gas. It is emitted from the source of the low-rise model rooftop. The emission velocity ratio, $\bar{V}_g/\bar{U}_0=0.05$, is considered low enough not to effect the flow.

2.6 Method of measurement

Figure 6 shows schematically the gas sampling and the wind velocity analysis system.

(1) Concentration measurement

The gas is simultaneously sampled at 8 points around models and led through 8 tubes into the multisampling apparatus. Then, the sampled gas is analyzed by the hydrocarbon analyzer. The averaging time is 3 minutes.

(2) Wind velocity measurement

The hot-wire anemometer is used for the

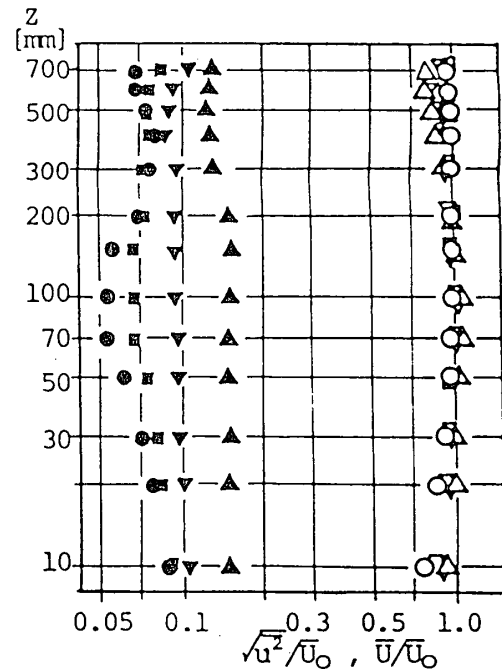


Fig. 5 Vertical wind velocity and turbulence intensity profiles of oncoming flow

without grid	\bar{U}/\bar{U}_0	$\sqrt{u^2}/\bar{U}_0$
2m	△	▲
3m	▽	▼
5m	□	■
without grid	○	●

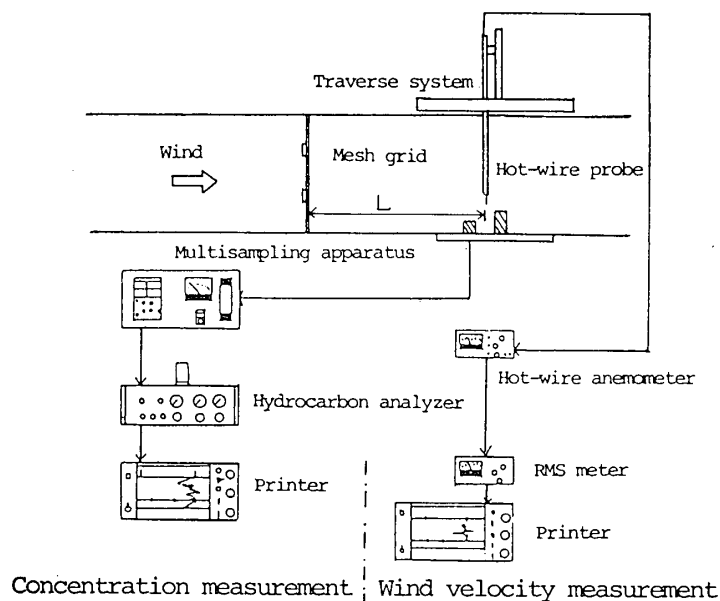


Fig. 6 Schematic of gas sampling and wind velocity analysis system

wind velocity measurement. Before the horizontal wind velocity is measured, the wind directions at each measuring point are determined by observing the movement of the flags set at the points. Then, the hot-wire probe is directed to coincide with the wind direction. The averaging time is 1 minute. The turbulence intensity is analyzed by a RMS meter, which is capable of calculating the standard deviation of the signal fluctuation.

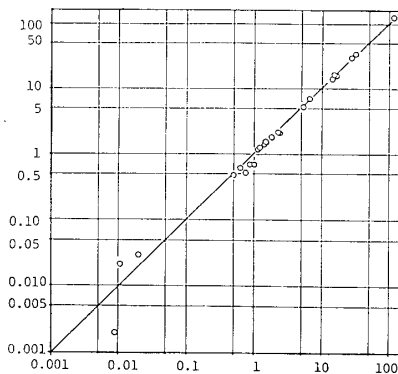
The vertical wind velocity is also measured by keeping the hot-wire probe angle constant. The wind directions are measured by observing the movement of a dandelion.

3. RESULTS AND DISCUSSION

3.1 Accuracy of concentration measurement

Figure 7 shows the reproductivity of the

C_{*1} (measured on October 6, 1983)



C_{*2} (measured on October 7, 1983)

Fig. 7 Reproductivity of concentration measurement for low-rise model

concentration measurement in case of the low-rise model. The reproductivity is defined as

$$Ec = \left(1 - \frac{1}{N} \cdot \sum |(C_{*2} - C_{*1}) C_{*1}|\right) \times 100$$

where C_{*1} : normalized concentration

measured on October 6, 1983

C_{*2} : normalized concentration

measured on October 7, 1983

under the same experimental conditions as C_{*1}

N: number of sampled data

The reproductivity is obtained more than 92.9%, which is considered to be accurate enough to measure concentrations around models.

3.2 Concentration distribution

Figures 8 and 9 show the normalized concentration distributions for $\sqrt{u^2_0}/\bar{U}_0 = 7.1\%$ and 15.3% respectively.

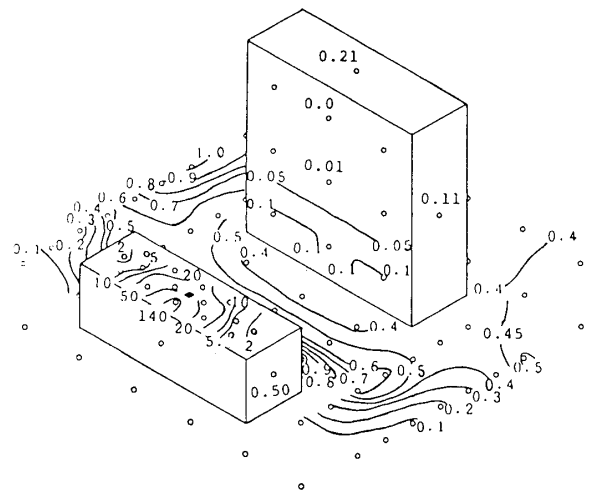


Fig. 8 Normalized concentration distributions for $\sqrt{u^2_0}/\bar{U}_0 = 7.1\%$

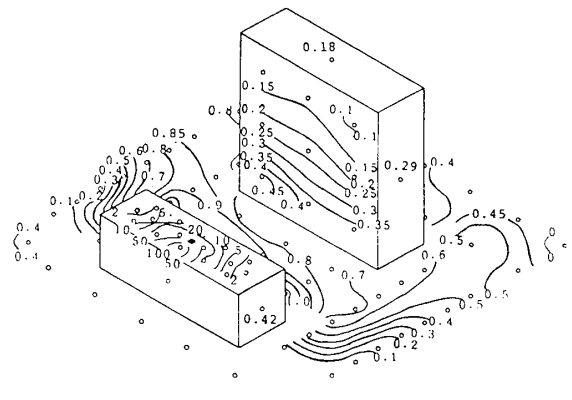


Fig. 9 Normalized concentration distributions for $\sqrt{u^2_0}/\bar{U}_0 = 15.3\%$

(1) On rooftop of low-rise model

It is found that the mean concentration on the rooftop for $\sqrt{u^2_0}/\bar{U}_0 = 15.3\%$ is approximately 20% lower than for $\sqrt{u^2_0}/\bar{U}_0 = 7.1\%$. The high concentration is found behind the source at the rooftop because the tracer gas im-

mediately reattaches on the rooftop by the eddy caused by the flow separating on the front edge of the low-rise model.

(2) On upwind face of high-rise model

The mean concentration on the upwind face of the high-rise model is not proportional to $\sqrt{u_0^2}/\bar{U}_0$. Also, driven by the stream flowing downward along the upwind face, the high concentration moves from the upper part to the lower part of the high-rise model.

(3) On ground surface

The concentration on the ground surface near the high-rise model increases as $\sqrt{u_0^2}/\bar{U}_0$ does. The mean concentration on the ground is higher than that on the upwind face of the high rise model.

(4) Dimensionless concentration difference

To judge whether the concentration distribution should be considered same, a dimension-

less concentration difference E_c is defined as follows.

$$E_c = \frac{100}{N} \cdot \sum [(C_{*i1} - C_{*i2}) / C_{*i2}]$$

where C_{*i1} : dimensionless concentration measured with mesh grid

C_{*i2} : dimensionless concentration measured without mesh grid

E_c comes small when the distribution patterns are same. This judging method is useful in determining the mean deviation from the standard distribution.

Figure 10 shows the relationship between E_c and $\sqrt{u_0^2}/\bar{U}_0$. With $\sqrt{u_0^2}/\bar{U}_0$ double, E_c for the concentration distribution on the rooftop of the low-rise model decreases 20%, while E_c increases 96% and 43% for the upwind face of the high-rise model and the ground surface between the models respectively.

3.3 Wind velocity distribution

(1) Horizontal distribution

Figures 11 and 12 show the results of the normalized horizontal wind velocity distributions around the models for $\sqrt{u_0^2}/\bar{U}_0 = 7.1\%$ and 15.3% respectively. It is found that the lengths of the cavity wake which stretch behind the high-rise model, are different each other. The lengths are determined by the wind di-

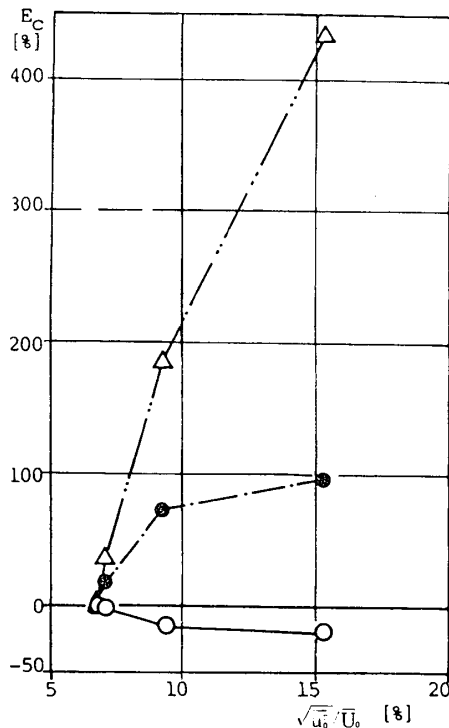


Fig. 10 Relationship between E_c and turbulence intensity of oncoming flow

- : on rooftop of low-rise model (16 points)
 ●: on ground surface between models (9 points)
 △: on upwind face of high-rise model (9 points)

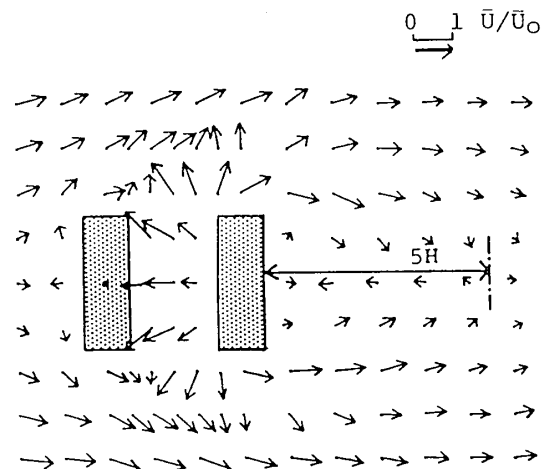


Fig. 11 Normalized horizontal wind velocity distribution for $\sqrt{u_0^2}/\bar{U}_0 = 7.1\%$

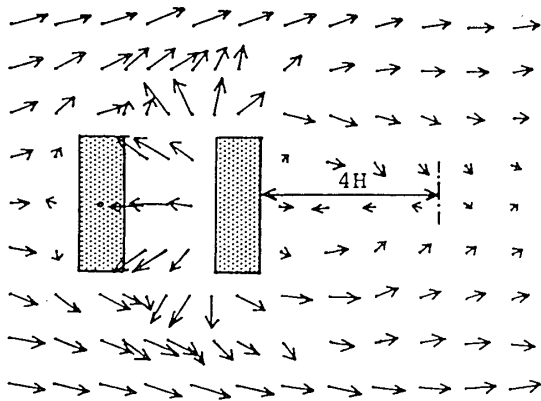


Fig. 12 Normalized horizontal wind velocity distribution for $\sqrt{u^2}/\bar{U}_0 = 15.3\%$

rection and velocity along $Y/H=0$. They are equal to $5H$ and $4H$ for $\sqrt{u^2}/\bar{U}_0 = 7.1\%$ and 15.3% respectively. It is therefore found that the length is in reverse proportion to $\sqrt{u^2}/\bar{U}_0$.

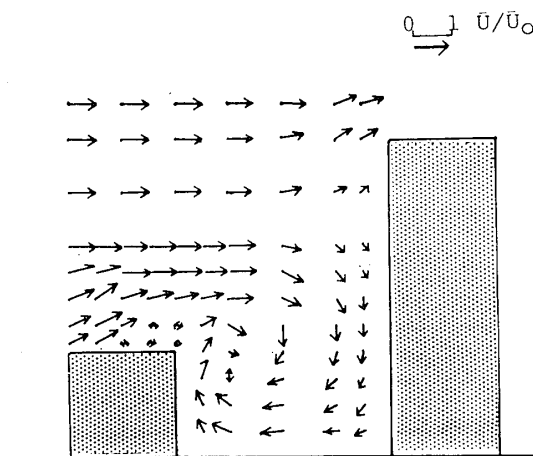


Fig. 13 Normalized vertical wind velocity distribution for $\sqrt{u^2}/\bar{U}_0 = 7.1\%$

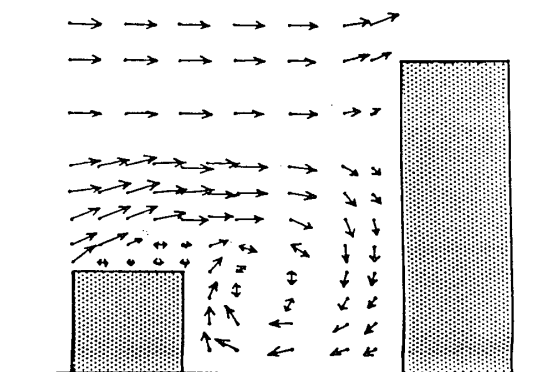


Fig. 14 Normalized vertical wind velocity distribution for $\sqrt{u^2}/\bar{U}_0 = 15.3\%$

(2) Vertical distribution

Figures 13 and 14 show the results of the normalized vertical wind velocity distribution for $\sqrt{u^2}/\bar{U}_0 = 7.1\%$ and 15.3% respectively. The wind direction which is impossible to determine is expressed using a sign of ' \leftrightarrow '. The large eddy is seen between the models and the small one is also seen above the rooftop of the low-rise model. It is found that even if the turbulence intensities of the on-coming flow are different each other, the vertical wind velocity distributions between models are same.

3.4 Turbulence intensity distribution

Figures 15 and 16 show the results of the

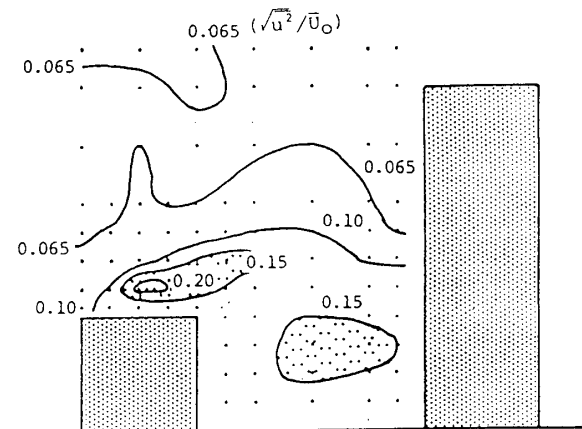


Fig. 15 Vertical turbulence intensity distribution for $\sqrt{u^2}/\bar{U}_0 = 7.1\%$

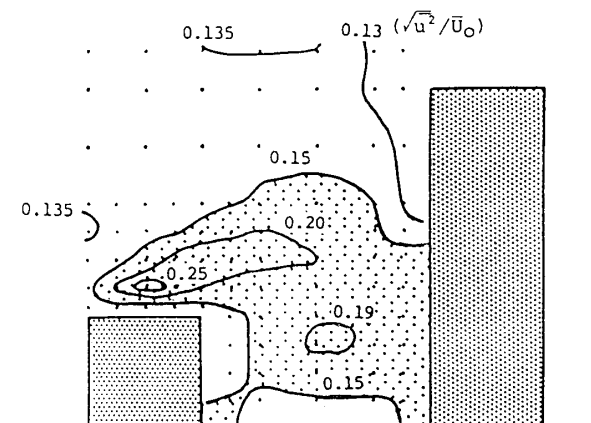


Fig. 16 Vertical turbulence intensity distribution for $\sqrt{u^2}/\bar{U}_0 = 15.3\%$

vertical turbulence intensity distribution. As can be seen from the Figures, $\sqrt{\overline{u^2}}/\overline{U}_0$ becomes large where the eddies are existed. Maximum turbulence intensity is seen near the rooftop of the low-rise model and equal to 25% for $\sqrt{\overline{u^2}}/\overline{U}_0=15.3\%$.

3.5 Dimensionless wind velocity and turbulence velocity differences

In order to determine the degrees of the differences both in the velocity and the turbulence intensity distributions, the differences are defined, like Ec, as follows;

for the wind velocity distribution

$$E\overline{U} = \frac{100}{N} \cdot \sum [(\overline{U}_{i1} - \overline{U}_{i2})/\overline{U}_{i2}]$$

where \overline{U}_{i1} : wind velocity measured with mesh grid

\overline{U}_{i2} : wind velocity measured without mesh grid

for the turbulence intensity distribution

$$Eu = \frac{100}{N} \cdot \sum [(\sqrt{\overline{u^2}_{i1}} - \sqrt{\overline{u^2}_{i2}})/\sqrt{\overline{u^2}_{i2}}]$$

where $\sqrt{\overline{u^2}_{i1}}$: turbulence intensity measured with mesh grid

$\sqrt{\overline{u^2}_{i2}}$: turbulence intensity measured without mesh grid

Figure 17 shows the results of $E\overline{U}$ and Eu calculated with the wind velocities and turbulence intensities measured between the models. Regardless of $\sqrt{\overline{u^2}}/\overline{U}_0$, $E\overline{U}$ is almost equal to 0. But, $\sqrt{\overline{u^2}}/\overline{U}_0$ effects very much on $\sqrt{\overline{u^2}}/\overline{U}_0$ around the models. Especially Eu measured on the vertical plane is equal to 90% for $\sqrt{\overline{u^2}}/\overline{U}_0$

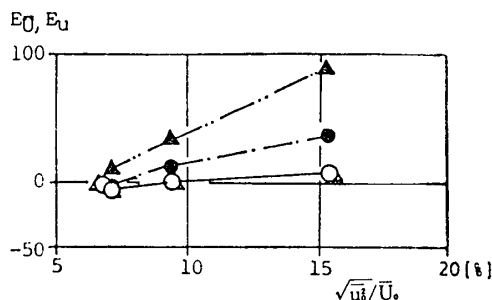


Fig. 17 Eu and $E\overline{U}$ for various $\sqrt{\overline{u^2}}/\overline{U}_0$

=15.3%.

4. CONCLUSIONS

By considering the results of concentration, wind velocity and turbulence intensity distributions, the following three conclusions are confirmed.

(1) The concentration on the rooftop of the low-rise model with the source increases as the turbulence intensity of the oncoming flow does. On the other hand, the concentrations on the upwind face of the high rise model and on the ground surface between the models, indicate the inverse inclination.

(2) The length of the cavity wake which stretches behind the high-rise model increases as the turbulence intensity of the oncoming flow does. It is approximately 4 H for $\sqrt{\overline{u^2}}/\overline{U}_0=15.3\%$.

(3) The vertical turbulence intensity distribution along $Y/H=0$ is proportional to the turbulence intensity of the oncoming flow.

Acknowledgements

We would like to express our thanks to Y. Iwakoshi, H. Nakai, K. Kitamura and M. Saitho for their help during the experiments.

References

- 1) J. Halitsky: 'Wind Tunnel Tests of Gas Diffusion from a Leak in the Shell of a Nuclear Power Reactor and from a Nearby Stack', Geophys. Sci. Lab. Rept. 63-2, Det. of Met. and Ocean, New York Univ., 1963.
- 2) N. Ukeguchi, H. Okamoto and Y. Ide: 'Wind Tunnel Experiments on Exhaust Gas Diffusion with Thermal Elevation', Second International Clean Air Congress, 1970.
- 3) W. G. Hoydysh and Ogawa: 'Characteristics of Wind Turbulence and Pollutant Concentration in and about the Model City', 67th Annual Meeting of the Air Pollution Control Association, 1974.
- 4) T. Shoda, S. Murakami, K. Uehara and M. Ohba: 'Wind Tunnel Experiment on Thermal Pollution by Exhaust Gas Emitted from District

- Heating Plant', Monthly Journal of Institute of Industrial Science (SESAN-KENKYU), Univ. of Tokyo, Vol.28, No.10, 1976.
- 5) J. E. Cermak: 'Laboratory Simulation of the Atmospheric Boundary Layer', AIAA, Vol.9, No.9, 1971.
 - 6) W. H. Snyder: 'Similarity Criteria for the Application of Fluid Models to the Study of Air Pollution Meteorology', Boundary-Layer Meteorology, No.3, 1972.
 - 7) D. P. Hoult, S. R. O'Dea, G. L. Touchton and R. J. Ketterer: 'Turbulent Plume in a Turbulent Cross Flow--Comparison of Wind Tunnel Tests with Field Observations', Journal of the Air Pollution Control Association, Vol.27, No.1, 1977.
 - 8) J. Golden: 'Scale Model Techniques', M.S. Thesis, College of Engr., New York Univ., 1961.
 - 9) M. Ohba and N. Kobayashi: 'Reynolds Number Effects on Wind Velocity Distributions around a Cubic Model', Report of the Annual Meeting of the Architectural Institute of Japan, 1976.
 - 10) M. Ohba and M. Kobayashi: 'Experimental Studies on Gaseous Diffusion around Two Model Buildings', Report of the Annual Meeting of the Architectural Institute of Japan, 1983.